(Appeared in *Tectonophysics*, **478**, 19-33, 2009)
doi: 10.1016/j.tecto.2009.02.035

Aeromagnetic constraints on the subsurface structure of Stromboli Volcano, Aeolian Islands, Italy

Shigeo Okuma [a], Christian Stotter [b], Robert Supper [c], Tadashi Nakatsuka [a], Ryuta Furukawa [a], and Klaus Motschka [c]

[a] *Geological Survey of Japan, AIST* (AIST Tsukuba Central 7, Higashi 1-1-1, Tsukuba 305-8567, Japan)
[b] (formerly c) *OMV Exploration and Production GmbH* (Gerasdorfer Straße 151, A-1210 Vienna, Austria)
[c] Geological Survey of Austria (Neulinggasse 38, A-1030 Vienna, Austria)

Received 30 November 2007; revised 29 December 2008; accepted 22 February 2009. Available online 10 March 2009.

Keywords: aeromagnetic, magnetic anomaly, magnetization, imaging, Stromboli Volcano

Abstract

Two helicopter-borne magnetic surveys were conducted over Stromboli Volcano and its surrounding areas on the Aeolian Islands, southern Italy in 2002 and 2004 to better understand the subsurface structure of the area. Observed data from those surveys were merged and aeromagnetic anomalies for Stromboli Island and its vicinity were reduced onto a smoothed surface, assuming equivalent anomalies below the observed surface. The magnetic terrain effects were calculated for the magnetic anomalies of the study area, assuming the magnetic structure comprised of an ensemble of prisms extending from the ground surface to a depth of 3000m below sea level: the average magnetization intensity was calculated to be 2.2 A/m for the edifice of Stromboli shallower than 1200m below sea level by comparing the observed and synthetic data. Next, apparent magnetization intensity mapping was applied to the observed anomalies using a uniform magnetization of 2.2 A/m as the initial value. The apparent magnetization intensity map indicates magnetic heterogeneities among volcanic rocks which constitute the edifice of the volcano. The most remarkable feature of the magnetization intensity map is a magnetization low which occupies the center of the island where the summit craters reside, suggesting demagnetization caused by the heat of conduits and/or hydrothermal activity in addition to the thick accumulation of less magnetic pyroclastic rocks. By comparing topographic and geologic maps, it can be seen that magnetization highs are distributed on the exposures of basaltic-andesite to andesite lavas (Paleostromboli I), shoshonitic lavas with an eccentric vent and a shield volcano (Neostromboli), on the south, north and west coasts of the volcano, respectively. These magnetization highs further extend offshore, implying the seaward continuation of these volcanic rocks. 3-D magnetic imaging was preliminarily applied to the same magnetic anomalies as well as for the magnetization intensity mapping. The result implies that the bottom depths of these magnetic structures are relatively shallow (<1500 m below sea level at the maximum). A distinctive regional magnetization high is distributed on a saddle area between Stromboli and Basiluzzo islands and extends to the two submarine eruptive centers on the southwestern submarine edifice of Stromboli. A careful examination on the results of the 2-D and 3-Dmagneticimaging implies that the saddle area is occupied by volcanic rocks from these eruptive centers and is also underlain by partially and/or completely concealed volcanic structures formed along a NW-SE direction conjugate to the main axis of regional tectonic trend in this area.

1. Introduction

The Aeolian Island Arc is located in the Tyrrhenian Sea, southern Italy and composed of seven volcanic islands: Alicudi, Filicudi, Salina, Lipari, Vulcano, Panarea, and Stromboli from west to east and several seamounts (Fig. 1). The volcanic activity of the islands is thought to originate from the subduction of the African Plate beneath the European Plate at the southern edge of the Tyrrhenian Sea (Gasparini et al., 1982). Since ancient Greek times, Stromboli in particular has been noted for its mild explosive eruptions which emit ash, lava fragments and volcanic bombs.

Due to its persistent and very regular activity and its relatively small size, Stromboli Volcano is an ideal study object or natural laboratory for volcanologists. Thus the volcano has been continuously observed and studied since the beginning of 19th century (e.g. Mercalli, 1891). Stromboli Island has been also investigated by a number of geophysical studies (Falsaperla and Schick, 1993). Geophysical investigations for volcanoes can be divided generally into two categories. Studies of the first category aim at investigating the internal structure of the volcanic edifice related to its activity. Studies in the second category strive to build physical models for Strombolian eruptions. Studies of the first category cannot be easily conducted on volcanic islands especially with steep flanks. In the first category, gravimetric studies were conducted on Stromboli by Bonasia and Yokoyama (1972) and Bonasia et al. (1973). The investigations revealed a Bouguer anomaly low in the very center of the island corresponding to low-density material filling the buried caldera.

The first geomagnetic survey was conducted as early as 1940 by Bossolasco (1943) with 218 measuring points distributed over Stromboli Island. Magnetic anomalies concentrate along a NE-SW line associated with recent activity. Further magnetic studies were conducted by Yokoyama (1959) and Casertano and Pinna (1971). In the 1970s, an aeromagnetic and gravity survey was conducted in the southern part of the Aeolian Islands by Iacobucci et al. (1977). In the 1980s, a regional airborne magnetic survey was conducted by Azienda Generale Italiana Petroli (AGIP) (1982). The magnetic anomalies were interpreted as an indication of the structural continuity between Stromboli and Panarea (Gabbianelli et al., 1993).

Since the 1990s, high-resolution aeromagnetic survey (HRAM) has made great progress with the development of GPS. HRAM is a practical tool for understanding shallow subsurface structures. Since the second half of the 1990s, HRAM has been applied for geologic hazard mitigation purposes such as earthquake and volcanic hazard mitigation (e.g. Okuma et al., 2001).

The Geological Survey of Austria (GBA) and Geological Survey of Japan, National Institute of Advanced Industrial Science and Technology (AIST) started airborne geophysical surveys on the Aeolian Islands in 1999 to better understand the subsurface structure of active volcanoes in the area. In addition to intensive studies in the Vulcano-Lipari volcanic complex (e.g. Supper et al., 2001, 2004; Stotter, 2005; Okuma et al., 2006a,b), aeromagnetic surveys were conducted over the area from Panarea to Stromboli in 2002 and over Stromboli Island and its vicinity in 2004 (Fig. 1) with a flight altitude of 100 m above terrain.

In this paper, we deal with these aeromagnetic surveys and the derived aeromagnetic anomalies of Stromboli Volcano. The results of apparent magnetization intensity mapping and preliminary 3-D magnetic imaging are also discussed with a special reference to the geologic structure compared with other geophysical data.

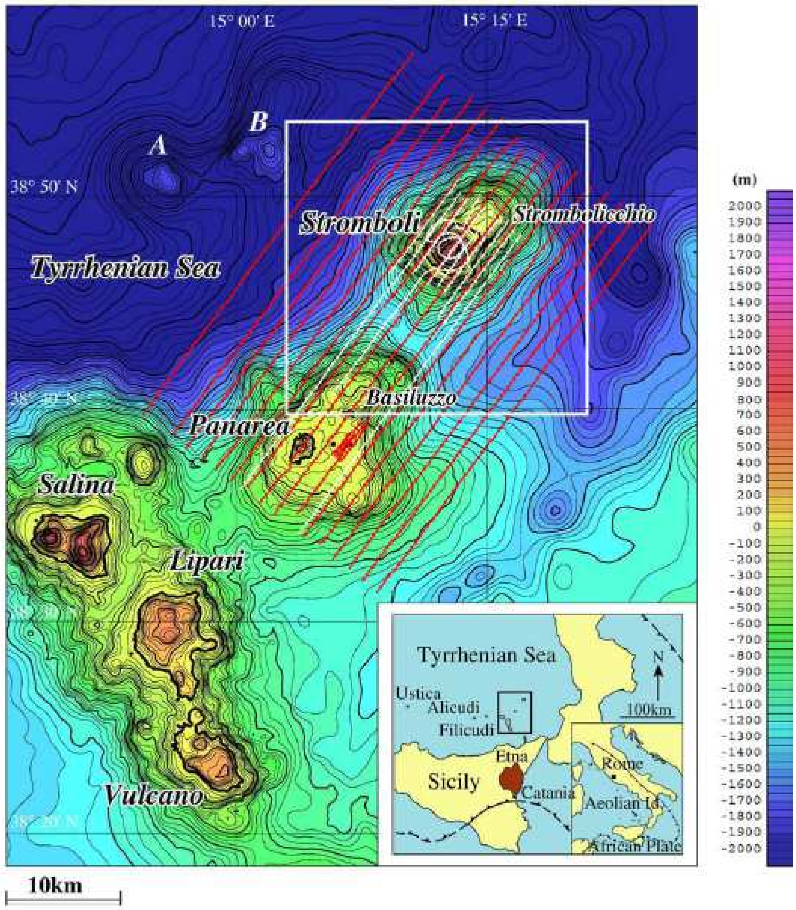

Fig. 1. Location map of study area. Red and white tick-marked lines indicate the 2002 and 2004 flight line paths, respectively. A rectangle shows the detailed study area of Stromboli Volcano and its vicinity, corresponding to the area in Fig. 5. A and B stand for the North A and North B seamounts by Gabbianelli et al. (1993), respectively. Topographic contour interval is 50 m. (For interpretation of the references to colour in this figure legend, the reader is referred to the web version of this article.)

2. Geologic settings

The geology of Stromboli Island has been discussed by several authors including Rosi (1980), Hornig-Kjarsgaard et al. (1993), Keller et al. (1993), Guest et al. (2003). Here, we follow a detailed chemical description from Hornig-Kjarsgaard et al. (1993). Deep focus seismicity shows hypocenters in the area of Stromboli at depths between 250 km and 300km in the area of Stromboli. The continental crust, on which the Aeolian Islands reside, thins out towards the center of the Tyrrhenian Basin and has a crustal thickness of about 18 km underneath Stromboli (Morelli, 1975). The age of the oldest products has been determined to 100 ka for Stromboli Island and 250 ka for the Strombolicchio volcanic neck (Gillot and Keller,1993). The latter is

Table 1 Chronological chart of Stromboli Volcano mainly based on Hornig-Kjarsgaard et al. (1993).

Unit	Radiometric age	Chemical composition
Recent Stromboli	6 ka–present	Shoshonitic (SHO), high-K calc-alkaline (HKCA)
Neostromboli	13–6 ka	Lc-shoshonitic (SHO) (Potassic, KS)
Vancori	25–13 ka	Shoshonitic (SHO)
Paleostromboli III and Scari	55–35 ka	High-K calc-alkaline to Shoshonitic (SHO)
Paleostromboli II	64–55 ka	Calc-alkaline (CA)
Paleostromboli I	100–64 ka	High-K calc-alkaline (HKCA)
Strombolicchio	200 ka	Calc-alkaline (CA)

likely to be the remnant of an older eroded volcanic edifice.

Seven major units can be identified on Stromboli (Table 1; see Fig. 2): the chemical rock composition of Stromboli varies from calc-alkaline (CA) to leucite-bearing (Lc-) shoshonitic or potassic (KS) through high-K calcalkaline (HKCA) and shoshonitic (SHO) with multiple recurrences throughout the history of the volcano. Between the calc-alkaline and shoshonitic rocks, all transitions occur. This could suggest the existence of a calc-alkaline parent magma which is frequently mixed with more potassic melts (Hornig-Kjarsgaard et al., 1993). The termination of three of these periods is marked by a distinct volcanic events associated with a change in the volcanic rock composition and/or eruptive behavior.

At the end of Paleostromboli I, a large crater depression formed, remnants of which can be found in an unconformity at 400m above sea level today. In the Paleostromboli III period, a large summit caldera developed, which was consequently filled with lava flows of the lower Vancori unit. The transition to the Neostromboli is marked by a large amount of lava flows that have run easily to the northwest, which implies that the northwest part of the upper Vancori crater had been removed at that time. Four onshore parasitic centers can be identified for the Neostromboli period:

1. Timpone del Fuoco (shield volcano, W coast)
2. Vallonazzo (eruptive fissure, NE)
3. Punta Labronzo (eccentric center, N coast)
4. Nell Cannestrá (eruptive fissure, NE).

A possible fifth parasitic cone offshore Ginostra is mentioned by Hornig-Kjarsgaard et al. (1993). Evidence on this offshore center comes from the Lazzaro tuffs. The transition from the Neostromboli to the recent Stromboli period is marked by a giant sector collapse and landslide, which formed today's active Sciara del Fuoco. This impressive NW flank of Stromboli is surrounded by dike swarms on both sides. An abrupt change in chemical rock composition can be also observed, which could be the effect of tapping a different magma reservoir. An eccentric volcanic

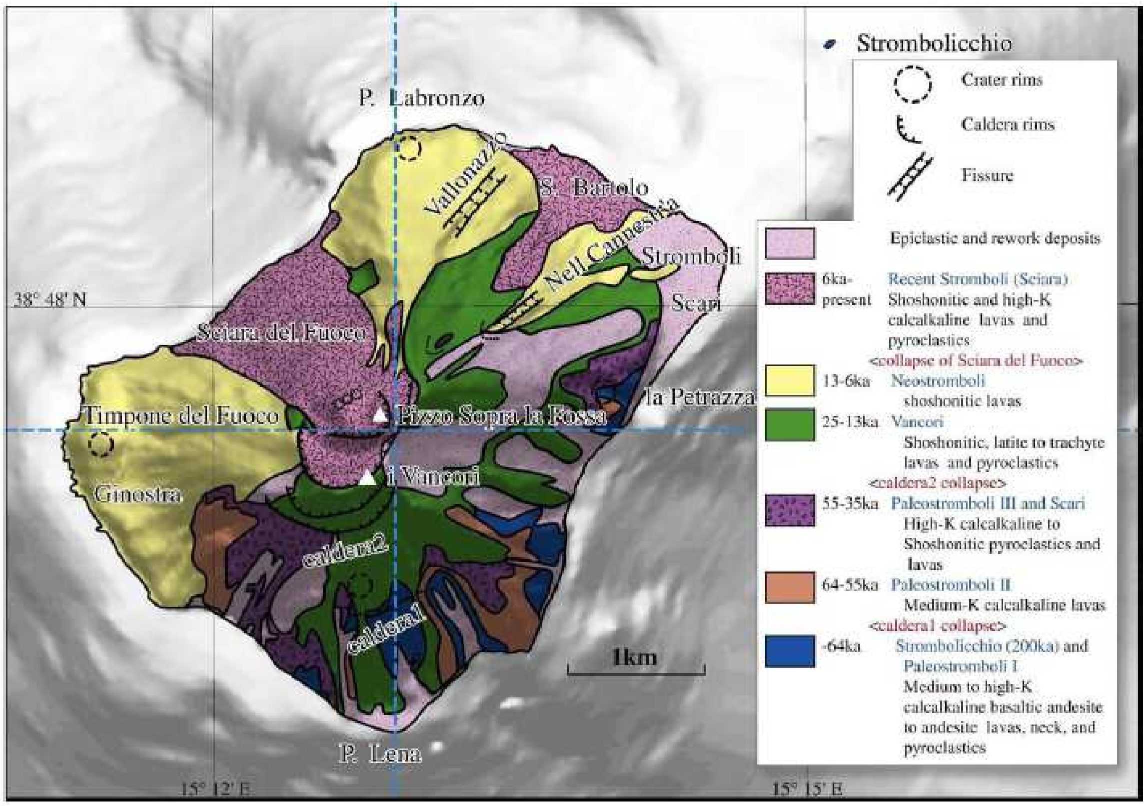

Fig. 2. Geologic map with a distribution of the major volcanic units of Stromboli Volcano. Simplified from Keller et al. (1993) and Guest et al. (2003). Topographic shading is superimposed. Vertical and horizontal blue dash lines indicate the locations of N-S and E-W cross-sections in Fig. 10, respectively.

center in the north developed in the recent Stromboli as well. Moderate explosive ejection of scoria, lapilli and ash, together with rare minor lava flows still frequently occurs at the active crater. A terrace within this crater at about 725 m above sea level hosts the three major vents. The mild volcanic activity as observed on Stromboli is generally named "Strombolian" activity.

3. Aeromagnetic surveys and reduction of magnetic anomalies on a smoothed surface

In 2002, a regional aeromagnetic survey was conducted over the area from Panarea to Stromboli, Aeolian Islands, southern Italy. The survey was flown by an AS350 B2 helicopter with a real-time DGPS navigation system along 17 survey lines spaced 1500m apart in a NE-SW direction at an altitude of 100m above the terrain and sea surface (Table 2; Fig.1). This survey was optimized to identify sources of submarine magnetic anomalies ～1000-1500 m below the surface. The magnetic sensor in a bird was suspended 30m below the helicopter. During the period of the 2002 survey a large submarine fumarolic vent opened in the area between Lisca Bianca and Dattilo offshore east of Panarea (Caracausi et al., 2005). In order to map the magnetic field during this extraordinary activity period, this area was covered by five additional flight lines, a few kilometers long, spaced approximately 200 m apart.

The total force magnetic field was measured using a Cesium magnetometer at a sampling rate of 10 Hz with a resolution exceeding 0.01 nT. The coordinates of the flight line path were determined using real-time DGPS. The helicopter was also equipped with an infrared sensor to detect the surface thermal signature related to volcanic activity. Diurnal magnetic variations were observed during the survey at a temporal base station near the heliport on Vulcanello, Vulcano.

In 2004, an additional survey was flown over Stromboli Volcano and its vicinity along 10 survey lines spaced 750 m apart and a single spiral line to avoid the on-going eruptive activity on Stromboli. The rest conditions are identical as the 2002 survey. The survey was designed to investigate the magnetic structure of subaerial volcanic rocks.

First, observed data of the 2002 survey were processed to find general characteristics of magnetic anomalies in the whole survey area. Corrections for diurnal magnetic variation and heading error were made (Okuma et al., 2003). The main field component from the tenth generation International Geomagnetic Reference Field (IGRF) (Maus and Macmillan, 2005) was also removed from the observed data.

Table 2 Outline of helicopter-borne magnetic survey over Stromboli Volcano and its surrounding areas conducted in 2002.

Survey period	November 3–November 6, 2002
Survey area	Refer to Fig. 1
Survey helicopter	Aerospatiale AS350 B2
Flight altitude	100 m above terrain or sea surface
Flight lines	Total 845 km, in NE–SW direction, 1500 m spacing
Navigation/flight path recovery	Visual flight aided by GPS/real-time differential GPS
Air base	Vulcanello, Vulcano, Aeolian Islands, Italy
Ground station	Vulcanello, Vulcano, Aeolian Islands, Italy 38°25′40″ N, 14°57′20″ E (ITRF)
Survey instruments	*Flight instrumentation* Airborne magnetometer: Scintrex CS-2 Cesium magnetometer with resolution more than 0.01 nT Data acquisition system: industrial PC with a LCD monitor GPS receiver: csi wireless DGPS MAX Laser altimeter: RIEGL LD-90-3300HR Infrared sensor: RAYTEC *Ground instrumentation* Ground magnetometer: Scintrex CS-2 Cesium magnetometer
Helicopter operation	ICARUS (Italy)

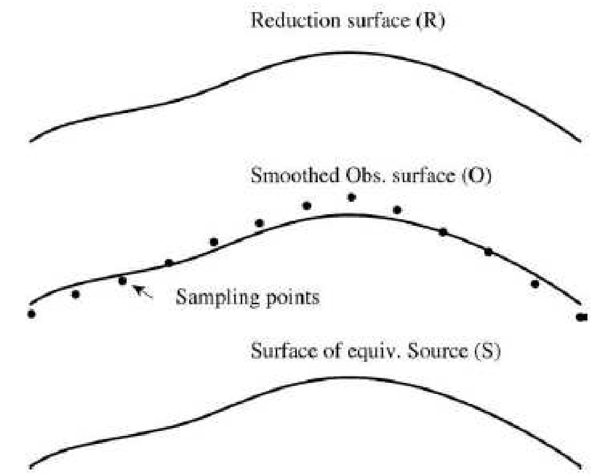

Fig. 3. Schematic framework of reduction by an equivalent-source technique. R, O and S are surfaces of reduction, smooth observation and equivalent source, respectively. Solid dots represent sampling points. Equivalent anomalies on the equivalent surface (S) are obtained by an iterative inversion using CG method and magnetic anomalies are calculated on the reduction surface (R) by upward continuation of the equivalent anomalies.

Total magnetic intensity anomalies on a smooth surface were calculated by a method that assumes equivalent anomalies below the observation surface (Nakatsuka and Okuma, 2006a). Data from points distributed randomly in three dimensions can be directly modeled with the conjugate gradient (CG) method to find a minimum-norm solution.

Initially, a smooth observation surface (O) (Fig. 3) was constructed by the method of 2-D weighted average for the random point altitude data. The surface of equivalent anomaly (S) was taken below and parallel to the O surface. Here the S surface should be lower than all the random data points. The surface of 300m above and parallel to the O surface was selected as the reduction surface (R) on which magnetic anomalies were calculated. Here the R surface is desirable to be lower unless the noise amplifying side effect of downward continuation from an actual observation point becomes distinct. However, some parts of the flight lines near Stromboli were flown at an altitude higher than the nominal altitude of 100 m above the terrain and sea surface (maximum clearance: 675 m) and consequently the surface mentioned above was selected. From the random data point observation data, a magnetic anomaly distribution on the S surface was extracted by the inversion method of the conjugate gradients (CG method). The iterative procedure of the reduction method was terminated when the rms of residuals of the observed and calculated field were 17.8 nT. The magnetic anomaly on the R surface (Fig. 4) was finally calculated from the above equivalent source magnetic anomaly distribution as a kind of upward continuation from a curved surface.

The total magnetic intensity anomaly map obtained from the data measured in 2002 (Fig. 4) indicates that a regional dipolar magnetic anomaly resides over Stromboli Volcano and its surrounding submarine topographic high, suggesting that the volcanic rocks of the volcanic edifice are magnetic. In contrast, no specific anomalies are generally dominant over the submarine topographic high on which Panarea and its surrounding islets lie, suggesting that the volcanic rocks of the area are not strongly magnetic. Exceptions are the areas of Panarea and offshore north of Basiluzzo. Panarea is a small part of a much larger submarine edifice whose overall shape is that of a truncated cone with an eastern protrusion (Fig. 1; Gabbianelli et al., 1990). A local magnetic high lies over Panarea, associated with outcrops of HKCA andesitic volcanic rocks on land (Hornig-Kjarsgaard et al., 1993). Another high is locally distributed offshore north of Basiluzzo. The difference of magnetic signatures between the Stromboli and Panarea areas is obviously caused by the petrologic difference between the volcanic rocks which compose each edifice: the general composition is basaltic to basaltic-andesitic for Stromboli (Hornig-Kjarsgaard et al., 1993), whereas andesitic to dacitic for Panarea (Calanchi et al., 1999).

A distinct magnetic high is distributed offshore between Stromboli and Basiluzzo. This area is underlain by a saddle of submarine topography with some minor submarine topographic lobs (Gabbianelli et al., 1993; Fig. 1). Although sufficient amplitude ranges are not seen in the magnetic map of the area because of the deep water depth (～1300 m below sea level), this magnetic high implies that these lobs are of volcanic origin. No specific anomaly was seen over submarine fumarolic areas between Lisca Bianca and Dattilo and that is to say a magnetically calm area is observed there.

Next, both data of the 2002 and 2004 surveys were merged to reveal characteristics of magnetic anomalies especially over Stromboli Volcano and its vicinity (Fig. 5(a)). A base level shift between the 2002 and 2004

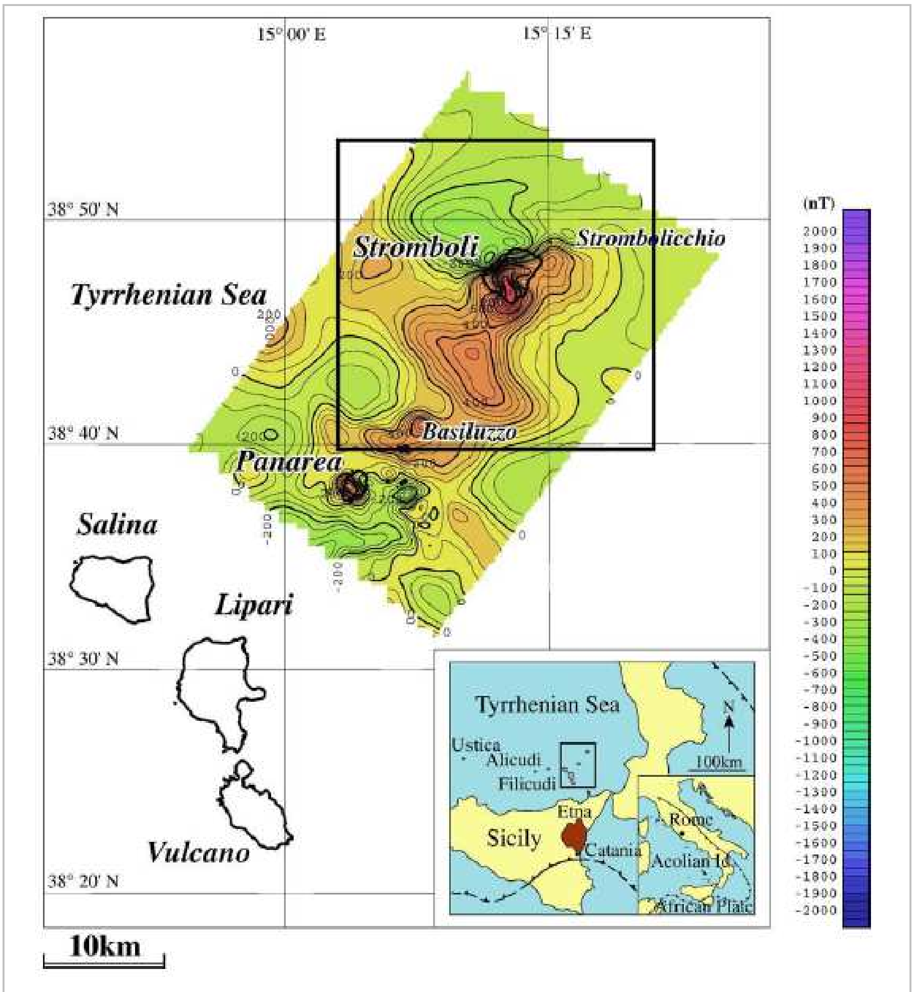

Fig. 4. Total magnetic intensity anomaly map of the Stromboli-Panarea volcanic complex on the surface 300m above and parallel to the smoothed observation surface (modified from Okuma et al., 2003). The data measured in 2002 were used. Contour interval is 50 nT. See also Fig. 1.

diurnal magnetic variations observed at the temporal base station was corrected using diurnal variations at the L'Aquila Geomagnetic Observatory at the Istituto Nazionale di Geofisica e Vulcanologia (INGV). Every other line was extracted from the 2004 survey to interpolate the line spacing of the 2002 survey into 750 m. A spiral line of the 2004 survey was also incorporated and processed with the other lines. However this spiral line was flown at an altitude higher than the other lines (maximum terrain and sea surface clearance: 1304 m) to avoid the on-going eruptive activity on Stromboli. To mitigate the amplifying downward continuation effect of the spiral line's data, a surface 550 m above and parallel to the smoothed observation surface (Fig. 5(b)) was selected as the reduction surface. The iterative procedure of the reduction method was terminated when the rms of residuals of the observed and calculated field were 25.5 nT.

Total magnetic intensity anomalies were reduced (Fig. 5(c)) onto the surface 550 m above and parallel to the smoothed observation surface, showing a magnetic high lying over the southern flank of Stromboli Volcano, as well as another high offshore of the northeastern edge of island. It suggests a terrain effect caused by volcanic rocks magnetized

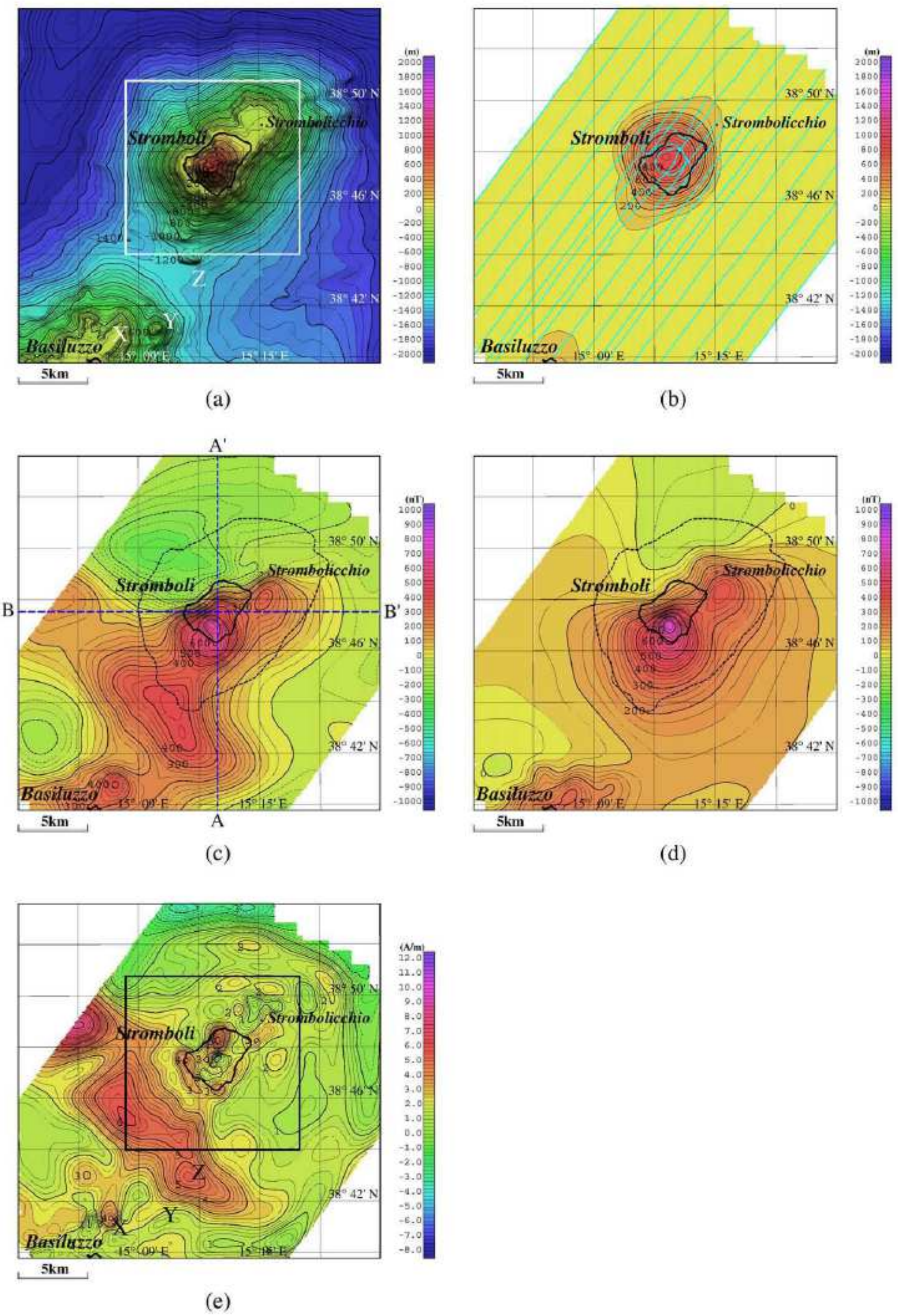

Fig. 5. **(a)** Topographic map of Stromboli Volcano and its vicinity. Contour interval is 50 m. A rectangle shows a close-up area of Stromboli Volcano, corresponding to the area of Fig. 6. X, Y and Z are referred to in the text. **(b)** Smoothed observation surface of the Stromboli aeromagnetic data by the method of 2-D weighted average for the random point altitude data. Contour interval is 50 m. Tick-marked lines show flight line paths. **(c)** Total magnetic intensity anomaly map of Stromboli Volcano and its vicinity on the surface 550 m above and parallel to the smoothed observation surface (b). Contour interval is 25 nT. Solid and dash lines indicate positive and negative values, respectively. A thick dash line indicates the bathymetric line of 1200 m below sea level and corresponds to the area for the calculation of an average magnetization intensity. A-A' and B-B' are locations of N-S and E-W cross-sections in Fig. 10, respectively. **(d)** Synthetic total magnetic intensity anomaly map of Stromboli Volcano and its vicinity on the surface 550 m above and parallel to the smoothed observation surface (b). The anomalies were calculated by the terrain model assuming a uniform magnetization of 2.2 A/m estimated by a statistical correlation method with a normal polarity (inclination: 54°, declination: 2°). See also Fig. 5(c). **(e)** Apparent magnetization intensity map of Stromboli Volcano and its vicinity. Contour interval is 0.25 A/m. See also Fig. 5(a).

in a direction parallel to the present Earth's magnetic field.

An average terrain magnetization was estimated using a statistical correlation method (Grauch, 1987; Nakatsuka, 1994). In this method, magnetization intensity J is calculated from the correlation coefficients of observed anomaly $f(x)$ and synthetic terrain effect $g(x)$ by

$$J = \sum_x \left(f(x) - \bar{f}\right)\left(g(x) - \bar{g}\right) / \sum_x \left(g(x) - \bar{g}\right)^2 \qquad (1)$$

where $\bar{f}$: average of f(x), $\bar{g}$: average of g(x), x denotes the position of observation.

The magnetic anomalies from the terrain effects were synthesized by an assembly of small prismatic bodies magnetized in the present Earth's magnetic field (inclination: 54°, declination: 2°) over the local area. Each prism has a horizontal dimension of 100 m by 100 m, extending from the ground surface to a constant depth. The depth to bottom of each prism was assumed to be a 3000 m below sea level from the result of a regional magnetic and gravity interpretation of the Aeolian arc (Barberi et al., 1994). They show the area is underlain by at least 3000 m of both effusive and intrusive volcanic formations (magnetic), which cover the metamorphic and sedimentary formations (non-magnetic) at depths greater than 3000-3500 m. However, it should be noted that the elevation of the bottom of the terrain model is arbitrary as long as it is below the lowest point (2450 m below sea level in this case) though the depth of 3000mwas adopted. Using any lower point would be equivalent to adding the magnetic effect of a horizontal slab, which is constant.

As the optimum magnetization intensity depends on the area chosen for calculation, careful examination is necessary to select it. It was calculated to be 2.4 A/m for the whole study area (Fig. 5(a)). The whole study area, however, includes positive anomalies near the southwest corner (Fig. 5(c)), which seem to have no relationship with Stromboli. To mitigate these anomalies, the optimum magnetization intensity was calculated to be 2.2 A/m for a limited area of Stromboli shallower than 1200m below sea level (Fig. 5(c) and (d)). This limited area represents the main edifice of the volcano projecting from the ocean bottom and is more suitable for the evaluation of an optimum magnetization intensity of Stromboli. Consequently, the value of 2.2 A/m was adopted. This value is similar to that of 2.0 A/m for Vulcano-Lipari volcanic complex (Okuma et al., 2006a) and lower than expected though more mafic rocks outcrop on Stromboli than on the Vulcano-Lipari complex. It is implied that the magnetic properties of the edifice of Stromboli are affected by the past and on-going volcanic activity of the volcano itself.

4. Apparent magnetization intensity mapping

Magnetization intensity mapping is a useful tool to evaluate surface geology and the shallow subsurface structure, as was demonstrated with reference to Izu-Oshima Volcano (Okuma et al., 1994) and the Vulcano-Lipari volcanic complex (Okuma et al., 2006a). Because of this, apparent magnetization intensity mapping (Nakatsuka, 1995) was applied to the observed magnetic anomalies (Fig.5(c)). Apparent magnetization intensities (Fig. 5(e)) were calculated assuming the same structure magnetized in the present Earth's magnetic field as that employed for calculating the terrain effect. The iterative procedure of the mapping method was started using a uniform magnetization of 2.2 A/m as the initial value, which was estimated in section 3. It should be stressed that the result of the inversion depends on the initial value to be selected. Because the method gives a minimum-norm solution which is the nearest to a starting model among probable solutions. Lacking other information on the alternative initial model, the uniform magnetization of 2.2 A/m was adopted. The iterative procedure was terminated when the rms of residuals of the observed and calculated field were 5.5 nT.

The resultant apparent magnetization intensity map (Fig. 5(e)) shows the general characteristics of magnetization intensities of Stromboli Volcano and its vicinity. A regional magnetization high trending NW-SE between Stromboli and Basiluzzo dominates the magnetization map with an intensity of 5-6 A/m. This high seems to extend northwestward to a seamount (North B Seamount, B in Fig. 1; Gabbianelli et al., 1993) 15 km offshore of the northwest Stromboli close to the survey area (Fig.1). Some parts of this high extend close to Stromboli and Basiluzzo. Local magnetization highs are present close to several marine topographic highs north and northeast of Basiluzzo (X and Y in Fig. 5(a)) but they are not likely to coincide with these topographic highs (Fig. 5(e)). A geologic interpretation of this regional high will be discussed in section 6. Local magnetization highs and lows lie over Stromboli and its surrounding submarine topographic highs ranging from 1 A/m to 5 A/m, with many magnetization anomalies aligned along a NE-SW trend.

Next the result of the magnetization intensity mapping is compared with the detailed topography of the close-up area of Stromboli. The detailed topographic map (Fig.

6 (a)) clearly shows that two topographic highs are linked to each other in a NE direction in the area: one is Stromboli and the other is an obvious abrasion platform with Strombolicchio on the top offshore northeast of Stromboli, which is attributed to the earliest phase of volcanic activity (Gabbianelli et al., 1993). Another abrasion platform lies between Ginostra and Punta Lena along the southwestern coastline of Stromboli. The apparent magnetization intensity map with the topographic shading of the same area (Fig. 6(b)) shows some relationships between the magnetization intensity and submarine topography of the area. An apparent magnetization low (<1 A/m; a in Fig. 6(b)) lies on an abrasion platform offshore of the northeastern volcano on which Strombolicchio resides, suggesting that the platform is underlain by less magnetic rocks such as pyroclastic rocks. Two sparker profiles across the shelf of the Strombolicchio area show volcano-sedimentary wedges, overlain by sub-horizontal deposits, at the northwestern margin (Gabbianelli et al., 1993). The deep structure (>∼100 m below ocean bottom) of the main part of the platform, however, is not clear because of multiple reflections and this low can be also ascribed to the altered center of the dissected edifice of an old volcano. On the contrary, some local magnetization highs (∼2.2A/m) are distributed at the western edge and northern slope of this abrasion platform, implying the remains of the dissected edifice.

In another comparison with a geologic map (Fig. 7), we can also see some interesting characteristics of magnetization intensities. It is clearly seen that Stromboli Island is fringed by several local magnetization highs of 3-5 A/m along the coastline (Figs. 5(e), 6(b) and 7). Two of them (4-5 A/m) range from the northern (∼5 A/m; e in Fig. 7) and western flanks (∼4 A/m; f in Fig. 7)) to each coastline. They correspond to the Neostromboli lava flows on the northern flank and at Punta Labronzo, an eccentric vent on the north coast, and Timpone del Fuoco, shoshonitic shield volcanoes (Neostromboli) on the west coast, respectively. Neostromboli lavas are the most potassic rocks on Stromboli, and the SiO_2 content of them is low (52%) (Hornig-Kjarsgaard et al., 1993), implying higher magnetic properties. Sciara del Fuoco is a huge depression that lies in between them with a weak magnetization high (∼3 A/m; g in Fig. 7). Whereas, several magnetic highs of 2-3 A/m (h, i and j in Fig. 7) are aligned along the eastern coastline and extend further NE offshore of Scari. Paleostromboli I rocks, HKCA andesite to basaltic-andesite, are partly outcropped in the coastal areas from Punta Lena to la Petrazza and

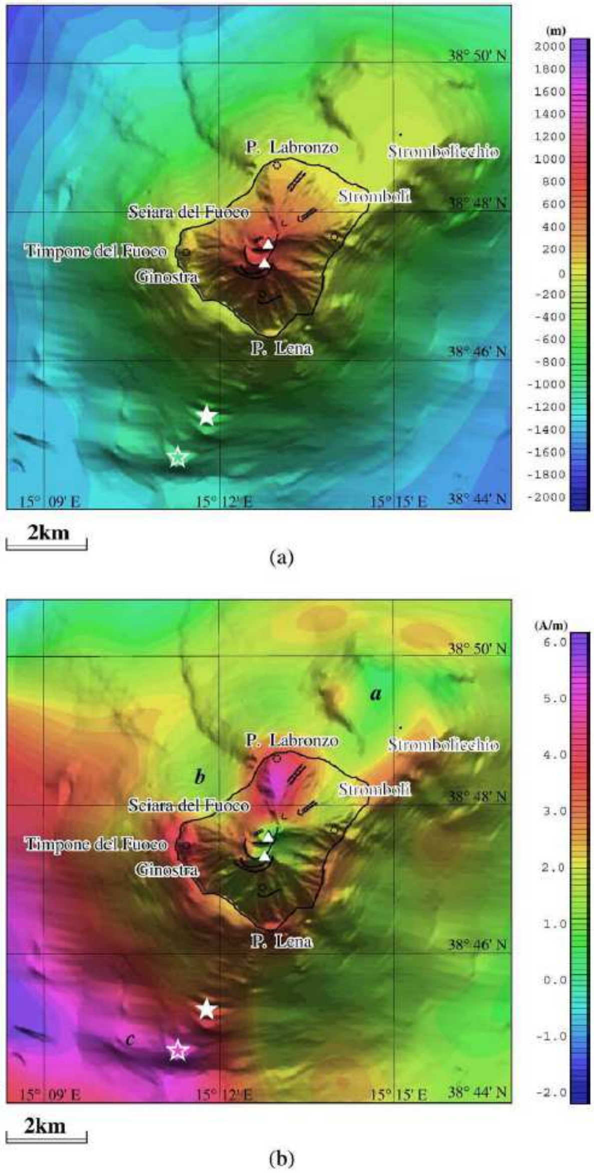

Fig. 6. **(a)** Shaded relief topographic map of the close-up area of Stromboli Volcano. Color contour interval is 50 m. Major geography and geologic features in Fig. 2 are superimposed. The white solid and open stars southwest of Stromboli indicate the approximate locations of the Cavoni and the Casoni seamounts (Gabbianelli et al., 1993; Gamberi et al., 2006), respectively. **(b)** Apparent magnetization intensity map of the close-up area of Stromboli Volcano with the topographic shading. Color contour interval is 0.1 A/m. Letters (a), (b) and (c) are referred to in the text.

estimated to compose Stromboli's base edifice. It is implied that the offshore extension of these highs is associated with the distribution of Paleostromboli I rocks at sea, aligned to a NE-SW direction, the main axis of the regional tectonic trend in this area.

The most obvious feature on Stromboli is a magnetization low (<1 A/m) which occupies the center of the island. As the summit craters cluster together, it is suggested that demagnetization was caused by the past and present volcanic activity. This matter will be

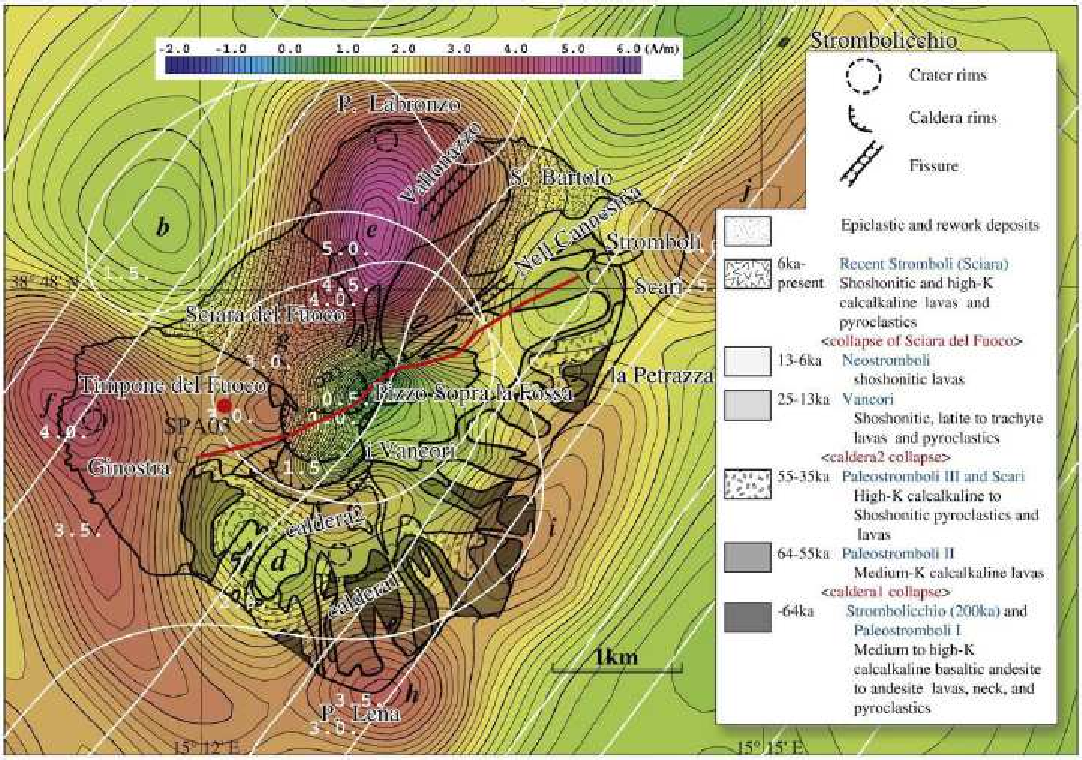

Fig. 7. Apparent magnetization intensity map of Stromboli Volcano superimposed on a geologic map of the volcano (Fig. 2). Contour interval is 0.1 A/m. See also Fig. 6(b). Tick-marked white lines show flight line paths. A red solid line of C-C' indicates the resistivity survey line by Finizola et al. (2006). Letters b, d and e-j are referred to in the text.

further discussed in section 6.

A local magnetization low (≈1.5 A/m; b in Fig. 6(b)) is centered approximately 1000 m offshore from the coastline of Sciara del Fuoco. This area corresponds to the submarine extension of Sciara del Fuoco, which extends further north to a depth of 1700 m below sea level and is morphologically as a depression (Romagnoli et al., 1993; Fig. 6(a)). This magnetization low implies the most of the debris, which used to constitute the preexisting slope, slid further north offshore without forming thick debris avalanche deposits when a flank failure occurred. Another magnetization low of approximately 1.5 A/m (d in Fig. 7) lies on the southwestern flank of the main edifice of the volcano, where Paleostromboli III rocks are mainly distributed (Fig. 7). Although no evidence has been obtained, the alteration of the volcanic rocks by the past hydrothermal activity might be one possibility to explain this magnetization low.

5. 3-D magnetic imaging

To limit the depth of the magnetic structure, a preliminary three-dimensional magnetic imaging (Nakatsuka and Okuma, 2006b) was conducted as a three-dimensional extension of the two-dimensional magnetization intensity mapping method (Nakatsuka, 1995).

Now, let k and i denote source position and observation point, respectively, then the magnetic anomaly Fi at a point i is given by

$$F_i = \sum_k G_{ik} J_k \quad (i = 1, 2, \cdots) \tag{2}$$

where G_{ik} is the geometric contribution factor of a source body at k to the magnetic anomaly at i, and J_k is the magnetization intensity of the source body at k. G_{ik} is calculated from the mathematical formula of the prism model. When we try to solve this equation by the use of the minimum norm property of CG method, most of the depth solutions tend to concentrate near the surface. To overcome this problem, a proper scaling (depth-weighting) can be applied to the Eq. (2) as follows.

$$J'_k = J_k / \alpha_k \,, \quad G'_{ik} = G_{ik} \cdot \alpha_k \tag{3}$$

$$F_i = \sum_x G'_{ik} J'_k \quad (i = 1, 2, \cdots) \tag{4}$$

Both Li and Oldenburg (1996) and Pilkington (1997) adopted $z^{3/2}$ (z: block depth from the observation surface) as a scaling factor to take into account of the effect of the amplitude decrease with the source depth. Portniaguine and Zhdanov (1999, 2002) used automatic scaling by means of a matrix normalization. On the basis of our preliminary test (Nakatsuka and Okuma, 2006b; Fig. 8), the scaling factor of z^1 gives almost exactly the same result as that of automatic scaling. The scaling factor of z^1 (i.e. automatic scaling) is more suitable selections for the scaling factor because the mean depth of the solution gives a good estimate of the source location for the model. This can be interpreted that the source effect decays with r^{-3} while the area of source effect increases with r^2 in the case of usual 2-D magnetic surveys. Fig. 8 indicates this situation of depth scaling in the 3-D magnetization imaging. Although the problem above can be mitigated by proper scaling, the solution still tends to have a wider extent than that of the model. Thus the thickness of the model estimated by this method should be treated as a maximum thickness.

3-D magnetic imaging was applied to the observed total magnetic intensity anomalies (Fig. 5(c)), assuming the same model as the magnetization intensity mapping but with three-dimensional variations of magnetization intensity allowed. The magnetic model with a flat bottom is composed of magnetic layers with a constant thickness of 500 m except the uppermost one and each layer consists of an ensemble of prism models with a horizontal dimension of 100 m by 100 m. The iterative procedure of the imaging method was started using a uniform magnetization of 2.2 A/m as the initial value and terminated when the rms of residuals of the observed and calculated field were 4.3 nT.

Figs. 9 and 10(a) and (b) indicate depth slices and cross-sections as the result of the imaging, respectively. It is obvious from Fig. 9 that magnetization highs of a long wavelength, estimated by apparent magnetization intensity mapping, were imaged as similar broad magnetic structures on the depth slices from −3000 m to −1500 m. Local magnetic highs and lows were imaged on the depth slices from −1000 m to 500 m, suggesting the heterogeneity of the Stromboli edifice structure.

According to the N-S cross-section of the profile A-A' (Fig. 10(a)), the bottom depths of high magnetization areas of Punta Labronzo, on the north coast, and Punta Lena, on the south coast, seem to be shallower than 1500 m below sea level. A low magnetization area ranges from the surface to 500 m below sea level below the summit. On the E-W cross-section of the profile B-B' (Fig. 10(b)), a high magnetization area ranges from the surface to 1500 m below sea level on the west coast around Timpone del Fuoco. These magnetization intensities can vary according to the thickness of the magnetic model. For instance, magnetization highs observed in Fig. 10(a) and (b) increase in amplitude by around 10% when the bottom depth of the model is

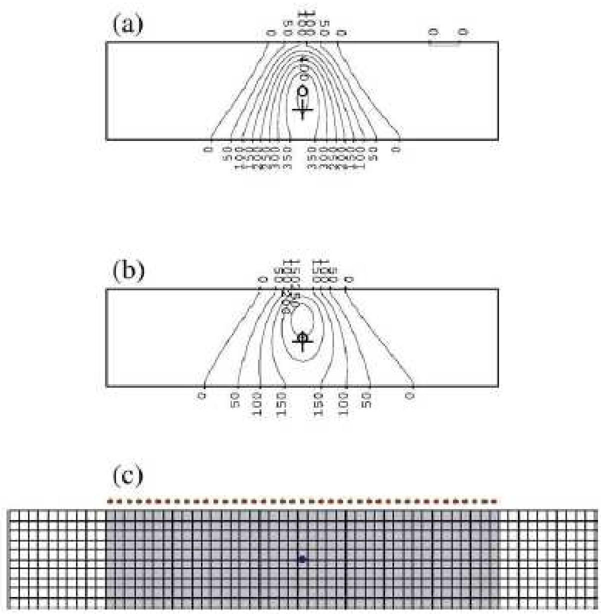

Fig. 8. Vertical cross-section of a preliminary test of synthetic model 3-D magnetization imaging (after Nakatsuka and Okuma, 2006b). A point dipole (or sphere) source is located at a depth of 500 m (shown by a circle) in the center of the area and has a magnetic moment of 1×10^9 Am^2 (=1 A/m×1 km^3) dipped at 45°, and 41×41 observation points on a 100 m square mesh are distributed as shown by dots on the bottom panel (c). The theoretical anomaly at these observation pointswas put into 3-D imaging analysis assuming 61×61×10 possible small source blocks (100m cubes) also cover the surrounding zone. The bottom panel (c) shows the vertical cross-section profile of the situation, and the panels (a) and (b) are the results from the scaling factor $r^{3/2}$ and automatic scaling by the matrix normalization as was suggested by Portniaguine and Zhdanov (1999, 2002). Contour interval is 50×10^{-2} A/m. Both results reveal awidely spread distribution especially downward. The cross marks indicate the locations of the center of mass (magnetization) for the anomalous range (exceeding half the peak value). It is obvious that the adoption of the scaling factor of $r^{3/2}$ gives a fairly deeper result considering the average depths.

changed to 2500 m below sea level from 3000 m.

To fully estimate the effect of the thickness of a magnetic model used for the 3-D imaging, we employed an alternative terrain model which has a bottom surface parallel to the terrain surface. This model, with a total thickness of 1000 m, consists of four sub-layers with a constant thickness of 250m each and top and bottom surfaces parallel to the terrain surface. Each layer is composed of small prismatic bodies with the same specification as was used in the case of the terrain model with a flat bottom. The same 3-D imaging method was applied to the observed magnetic anomalies (Fig. 5(c)) using a uniform magnetization intensity of 6.0 A/m as the initial value, which is an average magnetization calculated by the Eq. (1) for the limited area (Fig. 5(c) and (d)). Fig. 10(c) and (d) show the N-S and E-W crosssections of the result of the imaging respectively with the rms residuals of 3.9 nT. Magnetization intensities further increase at most of all the highs and lows but the general distribution pattern is unchanged. Magnetization highs of Punta Lena, Punta Labronzo and Timpone del Fuoco are analyzed to be ～6.0A/m, ～8.0 A/m and ～6.5A/m, respectively. Magnetization highs on the southwestern sea bottom in Fig. 10(c) and (d) become ～8.0A/m and ～6.0A/m, respectively. Whereas, a magnetization low at the summit area is ～1.5 A/m. In addition, the highest magnetization among the overall 3-D distribution of this model is approximately 9.4 A/m. These high values (≈8.0 A/m) are comparable with an average magnetization of 8 A/m assigned for Vulcanello on Vulcano from a rock magnetic study (Zanella and Lanza, 1994), where tephrites predominate (Keller, 1980). As the volcanic rocks on and around Stromboli fall within the same rock series ranging from arc-tholeiitic basalts through calcalkaline to shoshonitic lavas as on Vulcano (Gabbianelli et al., 1993), magnetization intensities of volcanic rocks on Stromboli can be expected to be similar to those on Vulcano. In case of reducing the thickness to 750 m, higher intensities exceeding 10 A/m were imaged in the areas of magnetization highs already analyzed. There is no evidence that such strongly magnetic rocks dominant in this area. Consequently, the minimum thickness for the magnetic model which accounts for the magnetization highs on Stromboli and its vicinity is estimated to be 1000 m.

At any rate the high magnetization areas imaged on the southwestern sea bottom in these cross-sections lack accurate information about their bottom depths (Fig. 10(a) and (b)). To improve the estimation of the extent by imaging, focusing inversion (compact inversion) (Portniaguine and Zhdanov, 1999) will be one of promising ways, though further studies are necessary.

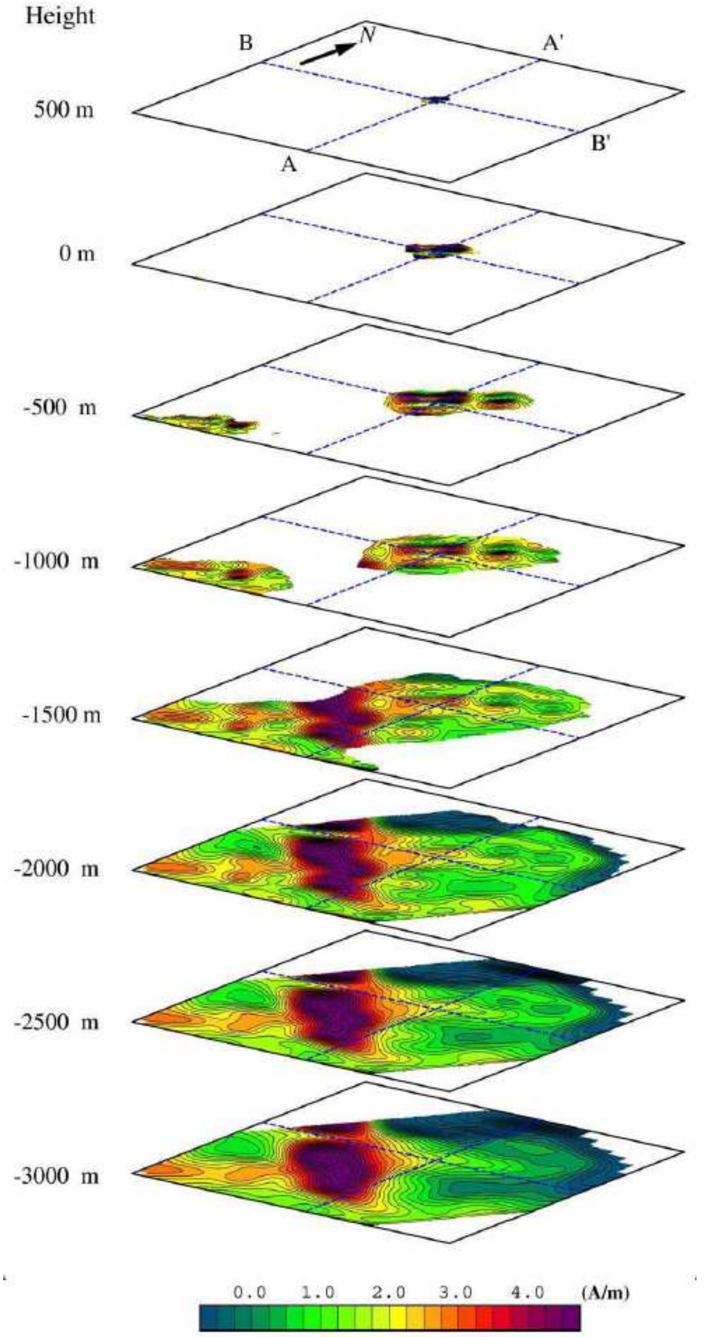

Fig. 9. Depth slices of the result of 3-D magnetic imaging of Stromboli Volcano and its vicinity. The depths in the map represent the bottom depths of each layer. The magnetic structure was assumed to be composed of eight layers of 500m thick except the uppermost one and the study area is 26.0 km×25.5 km large. Contour interval is 0.25 A/m. A-A' and B-B' are locations of N-S and E-W cross-sections in Fig. 10, respectively.

6. Discussions

Magnetic anomalies of Stromboli Volcano were merged from the data of 2002 and 2004 aeromagnetic surveys. The results of a magnetization intensity mapping and a 3-D magnetic imaging for Stromboli indicate magnetic heterogeneities of the volcano's edifice. However there are limited rock magnetic measurements on Stromboli, which are comparable with the results of the 2-D and 3-D imaging. Recently, paleomagnetic studies have been initiated to estimate the very recent volcanic activity of Stromboli. Speranza et al. (2004)

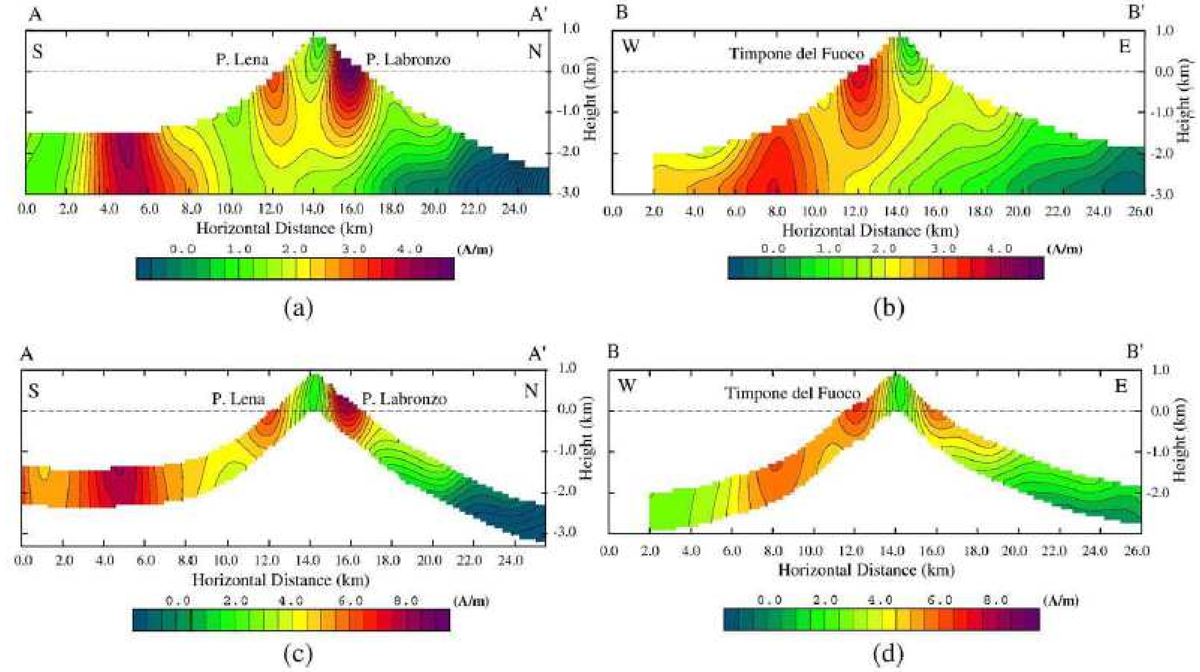

Fig. 10. Cross-sections of the result of 3-D magnetic imaging of Stromboli Volcano and its vicinity. (a) N-S cross-section and (b) E-W cross-section of the result of 3-D magnetic imaging of Stromboli Volcano and its vicinity (Fig. 9), assuming the terrain model which has a flat bottom depth of 3000 m below sea level. Vertical exaggeration is 1.25. Contour interval is 0.25 A/m. (c) N-S cross-section and (d) E-W cross-section of the result of 3-D magnetic imaging, assuming an alternative terrain model which has a bottom surface parallel to the terrain surface with a total thickness of 1000 m. Vertical exaggeration is 1.25. It is noted that contour interval is 0.5 A/m. Fig. 10(a) shows that the bottom depths of high magnetization areas of Punta Labronzo, on the north coast, and Punta Lena, on the south coast, seem to be shallower than 1500 m below sea level. A low magnetization area ranges from the surface to 500 m below sea level below the summit crater area. Fig. 10(b) indicates that a high magnetization area ranges from the surface to 1500m below sea level on the west coast around Timpone del Fuoco. Figs. 10(c) and 10(d) denote higher magnetization intensities than the terrain model with a flat bottom (Fig. 10(a) and 10(b)).

conducted paleomagnetic measurements of 17 spatter lavas from Stromboli Volcano and showed that most of the spatter lavas were formed after the 15th century. Only two measurements of the Natural Remnant Magnetization (NRM) intensity, however, were available in their paper: 4.1 A/m and 7.6 A/m for the samples collected from the same sampling site on the western flank (SPA03; a cross in Fig. 11). These values are similar to the magnetization intensities obtained by apparent magnetization intensity mapping: i.e. 5.0 A/m on the northern flank and 4.0 A/m on the Timpone del Fuoco on the west coast (Figs. 5(e), 6(b) and 7). However, the spatter samples were collected only from the very recent volcanic deposits and are not representative geologies where they are distributed. It is necessary to collect rock samples, which represent each geologic unit to obtain a statistical distribution of magnetization intensities like a study on the Vulcano-Lipari volcanic complex (Zanella and Lanza, 1994).

Concerning the magnetization low at the summit crater area (Figs. 6(b) and 7), it is suggested that the low is associated with the thick accumulation of less magnetic pyroclastic rocks within summit calderas. Actually Pizzo Sopra La Fossa, the second highest peak on Stromboli Island is a nested tuff cone within the calderas and might be treated as evidence of the geologic interpretation. However there are a limited number of other studies on the subsurface structure of Stromboli to support the interpretation, which were conducted from the ground-based surveys because of its hard access. Bonasia et al. (1973) conducted gravity measurements on the seven Aeolian Islands and compiled a Bouguer gravity map of Stromboli as well as the six other islands. A gravity low was located at the center of Stromboli (Fig. 11) and considered to have originated either by a buried caldera structure filled up with low-density materials, and/or by the open eruptive pipe. However, comparing the Bouguer gravity anomaly map of Volcano and Lipari volcanoes after terrain correction (Komazawa et al., 2002; Okuma et al., 2006a) and the map of the same volcanoes complied by Bonasia et al. (1973), it is suggested that terrain correction was not conducted on the latter map (Komazawa, personal communication). This implies that no terrain correction was also made for the gravity map of Stromboli (Bonasia et al., 1973). Consequently, it is questionable whether a gravity low occupies the center of Stromboli after terrain correction. As a result, the gravity low by Bonasia et al. (1973) cannot to be treated as direct evidence of the low-density materials occupying dominantly the center of the volcano.

In contrast, there is a possibility that the magnetization low was caused by the heat of conduits and/or a shallow magma chamber, as suggested by other geophysical data such as seismic observation. Seismic signals generated by the volcanic activity of Stromboli can be divided mainly into two types: volcanic tremor and explosion quakes (volcanic shocks) (Falsaperla and Schick, 1993). Volcanic tremor, which can be observed permanently, is thought to originate from pressure fluctuations induced by the flow of gas and magma within the volcano. There are strong indications that the source of these tremor signals is located not deeper than 300-400 m beneath the craters (Falsaperla and Schick, 1993). Whereas, explosion quakes are thought to be caused by degassing from magma head. Thus, their source locations can indicate the upper part of magma storage. Chouet et al. (2003) inferred that source-centroid locations of explosions are offset ～220 m beneath and ～160 m northwest of the active vents (Figs. 11 and 12), suggesting shallow magma storage.

Finizola et al. (2006) recently conducted geoelectrical, temperature, and CO_2 soil degassing investigations along a profile which crosses the island from SW to NE (Fig. 11). The shallow resistivity distribution (<200 m) of the island consists mainly of three resistive and three conductive sectors: the resistive parts are the lower part of the NE flank of the main edifice (R1), NE edge of the Neo-Stromboli caldera (R2) and SW flank (R3), while the conductive parts are the foot of the NE flank (C1), NE flank (C2) and inside the Neo-Stromboli caldera (C3) (Fig. 12). In general this pattern matches that of the magnetization intensities along the almost the same profile (Fig.12) and a magnetization low (≈1 A/m) on the summit area corresponds to the conductive layer C3, which represents low resistivities (≈ 100 Ω m). Finizola et al. (2006) also reported a strong relationship between resistivity, CO_2 measurements, temperature and self-potential. High values were observed for all the measurements except resistivity on the summit area close to Pizzo Sopra La Fossa, indicating the existence of a hydrothermal system. If so, the magnetization low

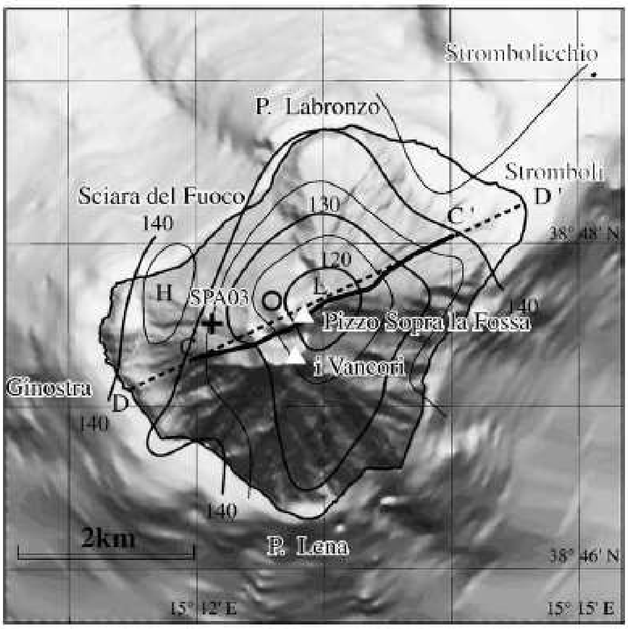

Fig. 11. Bouguer gravity map of Stromboli Volcano redrawn from Bonasia et al. (1973). Topographic shading is superimposed. Contour interval is 5 mgal. H and L signs denote gravity high and low, respectively. A solid line of C-C' indicates the resistivity survey line by Finizola et al. (2006). A dash line of D-D' shows the location of the cross-section of the result of 3-D magnetic imaging of Stromboli Volcano and its vicinity (Fig. 12). An open circle represents the approximate source location of explosion earthquakes determined by Chouet et al. (2003). A cross of SPA03 denotes the location of a paleomagnetic sampling point by Speranza et al. (2004).

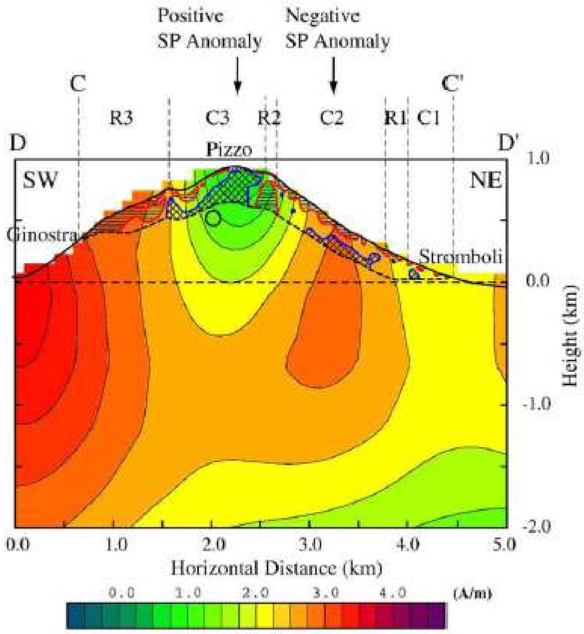

Fig. 12. Cross-section of 3-D magnetic imaging of Stromboli Volcano and its vicinity (Fig. 9) along the D-D' profile in Fig. 11. The area shallower than 2000 m below sea level was plotted. Vertical exaggeration is 1.25. Contour interval is 0.25 A/m. C1-C3 and R1-R2 are conductive and resistive parts of the edifice of Stromboli after Finizola et al. (2006). Crosshatched and striped parts correspond to the areas where show the resistivities lower than ≈100 Ω m and higher than 1400 Ω m, respectively (modified from Finizola et al. (2006)). An open circle represents the approximate source location of explosion quakes determined by Chouet et al. (2003).

which occupies the same area can be attributed to the demagnetization of volcanic rocks by hydrothermal alteration. A negative correlation between the magnetization intensity and resistivity is found on the NE flank of the main edifice of Stromboli (Fig.12): high magnetization intensities (≈2.5A/m)vs. low resistivities (<≈100 Ω m)at a depth. The negative SP anomaly without a temperature increase in the area implies that a cold aquifer accounts for the resistivity low (Finizola et al., 2006). The resistivity profile shows more detailed information on the subsurface structure of the volcano. Flight line spacing of our surveys, however, is too far apart to compare with their results (Fig. 7).

From these facts above, it is concluded that the magnetization low occupying the summit area can be attributed to demagnetization caused by the heat of conduits and/or hydrothermal activity as well as the thick accumulation of pyroclastic rocks.

Between Stromboli and Basiluzzo, a magnetization high with a long wavelength (c in Fig. 6(b)) occupies the narrow saddle area of marine topography deeper than 1000 m below sea level. According to a broad distribution of the magnetization high, it is suggested that the saddle area is underlain widely by volcanic products from its neighborhood. Two seamounts are known on the southwestern flank of the submarine edifice of Stromboli. Gabbianelli et al. (1993) spotted a peripheral submarine volcanic eruptive center (Cavoni seamount; white solid star in Fig. 6) at 700-800m below sea level. Samples taken from the Cavoni seamount were andesitic rocks of the high K_2O calcalkaline (HKCA) series attributed to the earliest phase of activity at Stromboli. Recently warm lavas and fresh scoriae were recovered from another seamount, Casoni seamount at 1000 m below sea level (white open star in Fig. 6), just southwest of the Cavoni seamount by dredging (Gamberi et al., 2006). This is evidence of the present submarine volcanic activity, both effusive and explosive, around the Stromboli Volcano. It is stressed that these seamounts are aligned along a NE-SW direction parallel to the main axis of regional tectonic trend of this area. As the regional magnetization high extends to these submarine eruptive centers, this high can be ascribed partly to volcanic products such as lava flows from these eruptive centers. Nevertheless, the uncertain bottom depths of the 3-D magnetic model (Fig. 10(a) and (b)) imply that this area is underlain by partially concealed magnetic structures with their tops projecting from the ocean floor as seamounts.

In the south of this area magnetization highs are also present offshore N and NE of Basiluzzo (Fig. 5(e)). As mentioned in section 4, they do not coincide with submarine topographic highs such as a NE trending prolonged ridge (X in Fig. 5(a)) and a suggested secondary eruptive center (Y in Fig. 5(a); Gabbianelli et al., 1993). Contrarily they seem to be associated with a submarine canyon west of the ridge and the northeast flank of the ridge respectively. They extend north and northeast to the main part of the regional high in the saddle area, implying the existence of volcanic rocks such as lava flows from a submarine eruptive center. Actually the ridge is accompanied by submarine fumarolic activity along the eastern edge (Gabbianelli et al., 1993), suggesting its volcanic origin.

As mentioned above, it is clear that the regional magnetization high has a close relationship with submarine secondary eruptive centers. However, 1000 m for the thickness of the magnetic model inferred from 3-D magnetic imaging (see in section 5) might be too thick to be attributable to the accumulation of volcanic rocks such as lava flows only from these secondary eruptive centers. In actual a maximum of 5 A/m at the southwestern part of this regional high (Z in Fig. 5(e)) does not accompany any topographic signatures (Z in Fig. 5(a)). A high magnetization area (～3.5 A/m in Fig.10(b)), which is a continuation of the regional high does not lie on the saddle area but on the western slope of Stromboli. Because of these, the regional magnetization high can be also attributed to fully conceal volcanic structures, which are aligned in a NW-SE direction conjugate to the main axis of regional tectonic trend in this area. This trend is almost parallel to a chain of volcanic islands (Salina, Lipari and Vulcano) in the southern part of the Aeolian Islands, in accordance with the strike of the Eolie-Tindari-Letojanni system (Barberi et al., 1994). In the Gioia Basin southeast of Panarea, several normal faults trending NW-SE are known (Barberi et al., 1994) and the saddle area seems to be a northwestern extension of one of the faults. Such a trend is evident as a subordinate tectonic direction on Panarea while it cannot be seen in geologic structures on Stromboli (Gabbianelli et al., 1993). On the basis of the above results, it is suggested that the saddle area is occupied by volcanic structures formed under a control of the regional tectonics in the area.

7. Conclusion

Aeromagnetic investigations were conducted to better understand the subsurface structure of Stromboli Volcano and its surrounding areas. On a regional scale, there is a difference between the distribution of magnetic anomalies over Stromboli and Panarea. More anomalies lie in the Stromboli area than in the Panarea area, associated with a different chemical composition of volcanic rocks, which constitute each area. Magnetization intensity mapping clearly indicates the magnetic heterogeneity of the volcanic edifice of Stromboli Volcano and its vicinity. The most obvious example is a magnetization low lying on the summit area, associated with the past and present volcanic and hydrothermal activity. Some magnetization highs correspond well to Neostromboli volcanic products such as lava flows, a shield volcano and an eccentric vent toward the coast. Preliminary 3-D magnetic imaging provided a rough constraint on the bottom depths of these volcanic products. In the offshore areas, a regional magnetization high is distributed between Stromboli and Basiluzzo islands and extends close to two seamounts (Cavoni and Casoni seamounts) on the southwestern flank of the submarine edifice of Stromboli, suggesting their volcanic origin. This implication is supported by the dredging of volcanic rocks from the two seamounts. These results demonstrate that magnetic surveys are useful to investigate the subsurface structure of active volcanoes on land and locate the extent of volcanic products by submarine volcanic activity.

Although our surveys were flown lower than the regional survey, the line spacing of 750 m we used was too far apart compared to the common specifications of today's high-resolution aeromagnetic survey over volcanoes (≈200 m). A high-resolution survey with narrower line spacing is necessary to determine a more detailed structure along with other data observed recently. Further improvement of magnetic imaging is also needed to properly focus on a solution.

Acknowledgements

This work was supported by the National Institute of Advanced Industrial Science and Technology (AIST), Japan and the Austrian Science Found, contract P15515-TEC "Improved Modeling and Interpretation of Complex Geophysical Data Applied to the Eolian Volcanic Province" (COMVOLC). Additional financial support was given by the Austrian Exchange Service (ÖAD) and the Istituto Nazionale di Geofisica e Vulcanologia, Italy (INGV). This work was also partly supported by the fellowship of Japanese Society for the Promotion of Science (JSPS) that was given to Christian Stotter. We express our gratitude to Maria Teresa Pareschi for providing the compilation of bathymetric data for the Aeolian Islands. We were grateful for receiving permission from the L'Aquila Geomagnetic Observatory at INGV to use their digital magnetic data for diurnal magnetic corrections. We especially appreciate Masao Komazawa for providing the information about the terrain correction of Bouguer gravity anomalies on the Aeolian Islands.

References

AGIP, 1982, Carta magnetica d'italia. anomalie del campo magnetico residuo, scala 1:500.000, foglio m. (in Italian).

Barberi, F., Gandino, A., Gioncada, A., La Torre, P., Sbrana, A., Zenucchini, C., 1994. The deep structure of the Aeolian Arc (Filicudi-Panarea-Vulcano sector) in light of gravity, magnetic and volcanological data. Journal of Volcanology and Geothermal Research, **61**, 189-206.

Bonasia, V., Yokoyama, I., 1972. Rilevamento gravimetrico di Stromboli (isole eolie). Rivista Italiana di Geofisica **21**, 109-113.

Bonasia, V., Luongo, G., Montagna, S., 1973. A land gravity survey of the Aeolian Islands. Bulletin of Volcanology **37**, 134-146.

Bossolasco, M., 1943. La distribuzione del campo magnetico terrestre all'isola di Stromboli. Pure and Applied Geophysics **5** (1-2), 11-36.

Calanchi, N., Tranne, C.A., Lucchini, F., Rossi, P.L., Villa, I.M., 1999. Explanatory notes to the geologic map (1:10,000) of Panarea and Basiluzzo islands (Aeolian arc. Italy). Acta Vulcanologica **11** (2), 223-243.

Caracausi, A., Ditta, M., Italiano, F., Longo, M., Nuccio, P.M., Paontia, A., 2005. Massive submarine gas output during the volcanic unrest off Panarea Island (Aeolian arc, Italy): inferences for explosive conditions. Geochemical Journal **39**, 459-467.

Casertano, L., Pinna, E., 1971. La recentle aativit dello Stromboli (febbraio-marzo 1954). Bollettino della Società Italiana Geofisica e Meteorologia **20**, 76-82.

Chouet, B., Dawson, P., Ohminato, T., Martinit, M., Saccorotti, G., Giudicepietro, F., De Luca, G., Milana, G., Scarpa, R., 2003. Source mechanisms of explosions at Stromboli Volcano, Italy, determined from moment-tensor inversions of very-long-period data. Journal of Geophysical Research **108** (B1), 2019. doi: 10.1029/2002JB001919.

Falsaperla, S., Schick, R., 1993. Geophysical studies on Stromboli volcano −a review. Acta Vulcanologica **3**, 153-162.

Finizola, A., Revil, A., Rizzo, E., Piscitelli, S., Ricci, T., Morini, J., Angeletti, B., Mocochain, L., Sortino, F., 2006. Hydrological insights at Stromboli volcano (Italy) from geoelectrical, temperature, and CO_2 soil degassing investigations. Geophysical Research Letters **33**, L17304. doi: 10.1029/2006GL026842.

Gabbianelli, G., Gillot, P.Y., Lanzafame, G., Romagnoli, C., Rossi, P.L., 1990. Tectonic and volcanic evolution of Panarea (Aeolian Islands, Italy). Marine Geology **92**, 313-326.

Gabbianelli, G., Romagnoli, C., Rossi, P.L., Calanchi, N., 1993. Marine geology of the Panarea-Stromboli area (Aeolian Archipelago, Southeastern Tyrrhenian sea). Acta

Vulcanologica **3**, 11-20.

Gamberi, F.,Marani,M., Landuzzi, V.,Magagnoli, A., Penitenti, D., Rosi, M., Bertagnini, A., Di Roberto, A., 2006. Sedimentologic and volcanologic investigation of the deep Tyrrhenian Sea: preliminary results of cruise VST02. Annals ofGeophysics **49**,767-781.

Gasparini, C., Iannaccone, G., Scandone, P., Scarpa, R., 1982. Seismotectonics of the Calabrian Arc. Tectonophysics **84**, 267-286.

Gillot, P., Keller, J., 1993. Radio chronological dating of Stromboli. Acta Vulcanologica **3**, 69-77.

Grauch, V.J.S., 1987. A new variable-magnetization terrain correction method for aeromagnetic data. Geophysics **52**, 94-107.

Guest, J., Cole, P., Duncan, A., Chester, D., 2003. *Volcanoes of Southern Italy*. The Geological Society, London. 304p.

Hornig-Kjarsgaard, I., Keller, J., Koberski, U., Stadlbauer, E., Francalanci, L., Lenhart, R., 1993. Geology, stratigraphy and volcanological evolution of the island of Stromboli, Aeolian arc, Italy. Acta Vulcanologica **3**, 21-68.

Iacobucci, F., Incoronato, A., Rapolla, A., Scarascia, S., 1977. Basement structural trends in the volcanic islands of Vulcano, Lipari and Salina (Eolian Islands, southern Thyrrenian Sea) computed by aeromagnetic and gravimetric data. Bollettino di Geofisica Teorica ed Applicata **73-74**, 49-61 XX.

Keller, J., 1980. The island of Vulcano. Rendiconti della Societa Italiana di Mineralogia e Petrologia **36**, 369-414.

Keller, J., Hornig-Kjarsgaard, I., Koberski, U., Stadlbauer, E. and Lenhart, R., 1993, Geological Map of Stromboli 1:10000, Acta Vulcanologica, **3**.

Komazawa, M., Okuma, S., Nakatsuka, T., Sugihara, M., Nakano, S., Furukawa, R., 2002. Gravity Survey of Vulcano and Lipari Volcano, Italy: Proceedings of the 106th SEGJ Conference, 254-257.

Li, Y., Oldenburg, D.W., 1996. 3-D inversion of magnetic data. Geophysics **61**, 394-408.

Maus, S., Macmillan, S., 2005. 10th Generation International Geomagnetic Reference Field. EOS **86** (16), 159.

Mercalli, G., 1891. Osservazioni fatte allo Stromboli nel settembre 1888 e nel febbraio-marzo 1889. Annali dell'Ufficio Centrale di Meteorologia e Geodinamica **10**,177-186.

Morelli, C., 1975. The gravity map of Italy. Quaderni de "La Ricerca Scientifica" **90**, 427-447.

Nakatsuka, T., 1994. Aeromagnetic anomalies over the area of Unzendake Volcano. Journal of Geomagnetism and Geoelectricity **46**, 529-540.

Nakatsuka, T., 1995. Minimum norm inversion of magnetic anomalies with application to aeromagnetic data in the Tanna area, Central Japan. Journal of Geomagnetism and Geoelectricity **47**, 295-311.

Nakatsuka, T., Okuma, S., 2006a. Reduction of magnetic anomaly observations from helicopter surveys at varying elevations. Exploration Geophysics **37**, 121-128.

Nakatsuka, T., Okuma, S., 2006b. 3D subsurface imaging by aeromagnetic data. Proc. of SEGJ 115th Conference, 196-199.

Okuma, S., Makino, M., Nakatsuka, T., 1994. Magnetization intensity mapping in and around Izu-Oshima Volcano, Japan. Journal of Geomagnetism and Geoelectricity **46**, 541-556.

Okuma, S., Nakatsuka, T., Morijiri, R., Makino, M., Uchida, T., Ogawa, Y., Takakura, S., Matsushima, N., 2001. Preliminary results of a high-resolution aeromagnetic survey over Usu Volcano, Hokkaido, Japan. Bulletins of the Geological Survey of Japan **52**, 149-154.

Okuma, S., Nakatsuka, T., Sugihara, M., Komazawa, M., Nakano, S., Furukawa, R., Elenjiparampil, E.J., Supper, R., Chiappini, M., 2003. Geophysical Signature on the Subsurface Structure of the Aeolian Islands, Italy, IUGG 2003 Abstracts, Week B, B.256.

Okuma, S., Nakatsuka, T., Komazawa, M., Sugihara, M., Nakano, S., Furukawa, R., Supper, R., 2006a. Shallow subsurface structure of the Vulcano-Lipari volcanic complex, Italy constrained by helicopter-borne aeromagnetic surveys. Exploration Geophysics **37**, 129-138.

Okuma, S., Nakatsuka, T., Supper, R., Komazawa, M., 2006b. High-resolution aeromagnetic anomaly map of the Vulcano-Lipari volcanic complex, Aeolian Islands, Italy. Bulletins of the Geological Survey of Japan **57**, 177-190.

Pilkington, M., 1997. 3-D magnetic imaging using conjugate gradients. Geophysics **62**, 1132-1142.

Portniaguine, O., Zhdanov, M.S., 1999. Focusing geophysical inversion images. Geophysics **64**, 874-887.

Portniaguine, O., Zhdanov, M.S., 2002. 3-D magnetic inversion with data compression and image focusing. Geophysics **67**, 1532-1541.

Romagnoli, C., Kokelaar, P., Rossi, P.L., Sodi, A., 1993. The submarine extension of Sciara del Fuoco feature (Stromboli isl.): morphologic characterization. Acta Vulcanologica **3**, 91-98.

Rosi, M., 1980. The island of Stromboli. Rendiconti della Societa Italiana di Mineralogia e Petrologia **36**, 1-24.

Speranza, F., Pompilio, M., Sagnotti, L., 2004. Paleomagnetism of Spatter lavas from Stromboli volcano (Aeolian Islands, Italy): implications for the age of paroxysmal eruptions. Geophysical Research Letters **31**, L02607. doi: 10.1029/2003GL018944.

Stotter, C., 2005, The Airborne Magnetic Method in Highly Magnetized Environment: Quantitative Analysis of Data From the Aeolian Islands Region, Ph.D. Thesis, University of Vienna, 223p.

Supper, R., Motschka, K., Seiberl, W., Fedi, M., 2001. Geophysical investigations in Southern Italian active volcanic regions. Bulletins of the Geological Survey of Japan **52**, 89-99.

Supper, R., De Ritis, R., Klaus, M., Chiappini, M., 2004. Aeromagnetic anomaly images of Vulcano and Southern Lipari Islands (Aeolian Archipelago, Italy). Annals of Geophysics **47**, 1803-1810.

Yokoyama, I., 1959. Sulla distribuzione del campo geomagnetico all'isola di Stromboli. Bollettino della Società Italiana Geofisica e Meteorologia **7**, 53-56.

Zanella, E., Lanza, R., 1994. Remanent and induced magnetization in the volcanites of Lipari and Vulcano (Aeolian Islands). Annali di Geofisica **37** (5), 1149-1156.